SPANDIDOS PUBLICATIONS

Comparative transcriptional study of the effects of high intracellular zinc on prostate carcinoma cells

POOI-FONG WONG[1] and SAZALY ABUBAKAR[2]

Departments of [1]Pharmacology, Faculty of Medicine, and [2]Medical Microbiology, Faculty of Medicine, University of Malaya, 50603 Kuala Lumpur, Malaysia

Received September 2, 2009; Accepted November 4, 2009

DOI: 10.3892/or_00000789

Abstract. The normally high concentration of zinc in normal prostate gland is significantly reduced in malignant prostate tissues, but its precise role in prostate tumorigenesis remains unclear. The present study investigates the growth and transcriptional responses of LNCaP prostate cancer cells to prolonged high Zn^{2+} treatment. Restoration of high intracellular Zn^{2+} to LNCaP cells significantly reduced the cell proliferation rate by 42.2±7.4% at the exponential growth phase and the efficiency of colony formation on soft agar by 87.2±2.5% at week 5 post-treatment. At least 161 LNCaP cell genes responded to the high intracellular Zn^{2+}, including ~10.6% genes that negatively regulate cell growth and ~16.1% genes that promote cancer cell proliferation. Inhibition of cell growth was transient as normal proliferation rate and colony formation efficiency were restored later even in the continuous presence of high intracellular Zn^{2+}. RT-qPCR showed constitutively higher expression levels of *FBL*, *CD164* and *STEAP1* in LNCaP cells. *FBL* and *CD164* were responsive to the treatment with Zn^{2+} in PNT2 prostate normal cells and were further overexpressed in the prolonged Zn^{2+}-treated LNCaP cells. These observations suggest that in general high Zn^{2+} has suppressive effects on prostate cancer cell growth but continuous exposure to an environment of high Zn^{2+} can lead to the overexpression of cancer promoting genes such as *FBL* and *CD164*. This could be the antagonistic mechanism used to overcome the initial cell growth inhibitory effects of high Zn^{2+}. These findings support a potential detrimental role of Zn^{2+} in prostate cancer.

Correspondence to: Dr Sazaly Abubakar, Department of Medical Microbiology, Faculty of Medicine, University of Malaya, 50603 Kuala Lumpur, Malaysia
E-mail: sazaly@ummc.edu.my; sazaly@um.edu.my

Abbreviations: *CD164*, CD164 sialomucin; *E2F3*, E2F transcription factor 3; *FBL*, fibrillarin; RT-qPCR, quantitative real-time reverse transcriptase PCR; *STEAP1*, six-transmembrane epithelial antigen of the prostate 1; TPEN, *N*, *N*, *N*', *N*'-tetrakis(2-pyridylmethyl)ethylenediamine

Key words: gene superinduction, microarray, trace element, tumorigenesis

Introduction

Zinc is an essential trace element important for various biological processes. Imbalance in Zn^{2+} homeostasis is associated with immunological disorders such as inflammation, diabetes, asthma, rheumatoid arthritis and Alzheimer's disease (1,2). It is also associated with pancreatic (3), prostatic (4) and esophageal squamous cell carcinoma (5). The diverse roles of this ion in regulating cell signal transduction pathways and gene expression perhaps plays a part in the development of these diseases. Microarray analyses on rat intestine (6) and liver tissues (7,8), human leukocyte subsets and lymphoblastoid cell (9-13), human colon adenocarcinoma cells (14), esophageal squamous cell carcinoma (5) and normal prostate epithelial cells (15) identified group of genes affected by changes in Zn^{2+} status. These include genes that regulate cell growth, metabolism, DNA repair, signal transduction, protein folding, energy production and genes that encode for heavy metal binding proteins, transporters, cytokines, cytokine receptors, adhesion molecules and T cells functions. These findings strongly support the regulatory roles of Zn^{2+} in cell growth and proliferation.

In a number of studies, Zn^{2+} is also reported to play important roles in the development and progression of prostate cancer. Its uniquely high concentration in the prostate gland is essential for the normal function of prostate cells and spermatozoa (16). Zn^{2+} is found significantly lower in malignant prostate tissues in comparison to the normal tissues (17). Zn^{2+} regulates the signal transduction pathways that are implicated in prostate tumorigenesis (18,19) and affects prostate cell growth and replication through various mechanisms (20-22). Whether Zn^{2+} regulates specific group of genes that are involved in prostate carcinogenesis or genes that increased malignant potentials in the cancerous prostate cells remained to be studied. In a recent study, we showed that high intracellular Zn^{2+} affected LNCaP prostatic cancer cell growth by modulating the ERK/VHR/ZAP70-associated pathways (23). The high intracellular Zn^{2+}, however, has no influence on the prostate cancer cell senescence nor apoptosis (24). In the present study, we simulated the effects

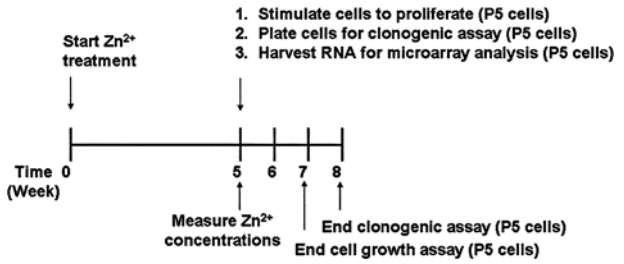

Figure 1. Schematic representation of timeline employed in the study. LNCaP prostate cancer cells were treated with Zn^{2+} for 5 weeks followed by subsequent analyses.

of progressive long-term intracellular Zn^{2+} accumulation by prolonged culturing of the LNCaP cells in growth medium supplemented with supraphysiologic concentration of Zn^{2+} and examined the effects on the prostate cancer cell growth and proliferation and on the Zn^{2+}-responsive genes.

Materials and methods

Cell culture and treatments. Human prostate cancer cells, LNCaP.FGC, were purchased from American Type Culture Collection (Rockville, USA). Human normal prostate epithelial cells, PNT2 were obtained as gift from Dr R. Rosli, Universiti Putra Malaysia. The cells were cultured in RPMI-1640 (Flowlab, Australia) supplemented with 10% FBS (Biowhittaker, USA), nonessential amino acid (1 mM), L-glutamine (2 mM) and 10 mM HEPES at 37˚C in humidified atmosphere of 5% CO_2. LNCaP cells were propagated in growth medium containing 1 or 10 μg/ml of $ZnSO_4$ for 5 passages in 5 weeks and subsequently analyzed as shown in the schematic timeline (Fig. 1). Control cell cultures were supplemented with only the Zn^{2+} diluent and propagated in parallel with the Zn^{2+}-supplemented cells. Cell proliferation rate and intracellular Zn^{2+} concentrations were measured as previously described (23). In separate experiments, short-term Zn^{2+} treatment was performed by incubating LNCaP and PNT2 cells with growth medium supplemented with 10 μg/ml Zn^{2+} for 2, 4, 8, 16, 24, 48 and 72 h. Control untreated cells were incubated up to 72 h. The influence of Zn^{2+} was also verified by treating cells with 100 μM *N*, *N*, *N*', *N*'-tetrakis(2-pyridylmethyl)ethylenediamine (TPEN), a known chelator of Zn^{2+}. At selected time points, total cellular RNA was harvested from the treated cells and stored until needed for quantitative real-time reverse transcriptase PCR (RT-qPCR).

Soft agar colony formation assay. LNCaP prostate cancer cells were treated with Zn^{2+} for 5 weeks. Cells were then assayed for anchorage-independent growth determined by their ability to form tumor colonies using soft agar colony formation assay. Single cell suspension was obtained by repeatedly passing cells through a 26Gx½' needle (Terumo, Japan). Five thousand cells were then resuspended in growth medium containing 0.3% agar (DNA grade agarose, Promega, USA). The cell suspension was layered on top of a base layer consisting of 0.5% agar prepared in growth medium in 60-mm plastic petri dishes (Falcon, USA). The cultures were incubated for 3 weeks at 37˚C in a humidified chamber supplied with 5% CO_2 in air. The growth medium was replenished every 3 days and cell colonies were counted after 3 weeks of incubation. Only colonies >0.5 mm were counted.

RNA extraction and target RNA preparation. Total cellular RNA of the Zn^{2+}-treated cells at the end of passage 5 (week 5) from representative experiments (n=3) was extracted from cells using TRI reagent® (Molecular Research Center, USA) and purified using RNeasy® Mini RNA Isolation Kit (Qiagen, Germany). Purified RNA integrity was checked by separating the RNA by electrophoresis in formaldehyde agarose gel. Complementary RNA (cRNA) amplification was then performed using Illumina® RNA Amplification Kit (Ambion, USA) according to the manufacturer's instructions. Approximately 100 ng of total RNA was reverse transcribed using the T7 oligo (dT) primer to prime cDNA synthesis. Following the second strand cDNA synthesis and column purification, *in vitro* transcription (IVT) was performed using biotinylated UTP to synthesize biotinylated cRNA. The cRNAs were column purified and used for hybridization. Illumina Human Ref Seq-8 Sentrix Bead Chip Arrays consisting of ~24,000 transcript probes (n=2 for control and n=3 for Zn^{2+}-supplemented cells) were hybridized with 850 ng biotinylated cRNA at 55˚C for 16 h. The arrays were washed, stained with strepavidin-Cy3 conjugate (2 μg/chip; GE Biosciences, USA) and scanned following the instruction for the Illumina BeadStation 500x (Illumina, USA).

Microarray data analysis. Microarray data were analyzed using the Genespring GX 7.3 (Agilent Technologies Inc., USA). Signal intensity values <0.01 were adjusted to the minimal intensity values of 0.01. Data were normalized to 50th percentile per chip and then to the median value per gene to compensate for experimental biases introduced by individual chip and differences in the detection efficiency between different spots. The raw data intensity values were then log transformed (log_2) to increase detection efficiency in discriminating differences between groups whose within-group variances are very different. Differential gene expression analysis was performed on Volcano plot using a cut-off fold change of 1.5 and parametric test with all available error estimates with Benjamini and Hochberg False Discovery Rate corrections (FDR of 0.05) (25). Hierarchical Clustering was performed on the normalized data using Genespring GX 7.3 (Agilent Technologies Inc.). Standard correlation was used as the dissimilarity estimates and average linkage method was used as the clustering algorithm. In the average linkage method, the distance between two clusters was calculated as the arithmetic mean of the distance between all possible pairs from the two clusters. Genes responsive to high intracellular Zn^{2+} were clustered based on biological process categories of the Gene Ontology Consortium (http://www.geneontology.org) using a web-based annotation program called NMC Annotation Tool (26).

Quantitative real-time reverse transcriptase PCR (RT-qPCR). Total cellular RNA of cells treated with Zn^{2+} for 2, 4,

Quantitative reverse transcriptase-polymerase chain reaction (RT-qPCR) amplification primer pairs used in the study.

Gene	GenBank accesion no.	Sequence (5'-3')	Polarity
CD164 antigen, sialomucin (CD164)	NM_006016	AACAGTTAGTGATTGTCAAGTGG CAGGTTGTGAGGTTGGAGTC	Sense Anti-sense
Complement component 1, q subcomponent binding protein (C1QBP1)	NM_001212	TGGCGAGTCTGAATGGAAGGATAC ATCTGTCTGCTCTACTGGCTCTTG	Sense Anti-sense
E2F transcription factor 3 (E2F3)	NM_001949	TGTCCCATCGTGCTTCCATTCC TCATCTGACCTGGTTCTCCTTTCC	Sense Anti-sense
Fibrillarin (FBL)	NM_001436	GAGGCTTTAGAGGTCGTG TCCACCATCACATTCTTCC	Sense Anti-sense
Metallothioneins 1 and 2 (MT1 and 2)	NM_005950 X97260	GCACCTCCTGCAAGAAAAGCT GCAGCCTTGGGCACACTT	Sense Anti-sense
Src homology 2 domain containing transforming protein 1 (SHC1)	NM_003029	TTGGGATAACAGAGGCAGGAGTG AAGGGAGGCAGGGCAGAGG	Sense Anti-sense
Six transmembrane epithelial antigen of the prostate 1 (STEAP1)	NM_012449	GCGAAGAGTGGGTGGCTGAAG GTGTGTGCTGAAGTTCTGAAGGG	Sense Anti-sense
Tumor-associated calcium signal transducer 1 (TACSTD1)	NM_002354	GAATAATAATCGTCAATGCCAGTG GCTCTCATCGCAGTCAGG	Sense Anti-sense
UDP glycosyltransferase 2 family, polypeptide B7 (UGT2)	NM_001074	GCAGCAGAATACAGCCATTGGATG TGAAGATGCCAGTACAGTCACCTC	Sense Anti-sense

8, 16, 24, 48, 72 h and those supplemented with Zn^{2+} for 5 weeks were isolated. RNAs were isolated using the TRI Reagent (Molecular Research Center) following the manufacturer's protocol. The RNA was treated with DNase and then 2 μg of it was reverse-transcribed using Super-Script™ II Reverse Transcriptase (Invitrogen, USA). RT-qPCR was performed using the SYBR-Green dye (Qiagen, UK) method on DNA Engine Opticon II (Bio-Rad, USA) with oligonucleotide primers shown in Table I. The primers were designed using Beacon Designer™ software (Premier Biosoft International, USA). Melt curve analysis was performed after each amplification followed by gel electrophoresis and DNA sequencing. Standard curves for internal standard (18S rRNA) and target genes were generated by linear regression using threshold cycle values, C_t versus log (standard dilutions). Amplification efficiency of the internal standard and target gene was determined in each run using the following equation: efficiency = $10^{(-1/slope)}$ -1. The initial copy number of the target gene in each sample (control untreated and Zn^{2+}-treated sample) was extrapolated from the standard curves. The initial target gene copy number was then normalized to the initial copy number of 18S rRNA in the respective sample. Fold-change in gene expression was calculated by dividing the normalized copy number of the target gene in the Zn^{2+}-treated sample with the normalized copy number of the target gene in the control untreated sample (27). RT-qPCR for all genes was performed in triplicates in at least three separate amplifications from 2 separate experiments. Data are presented as mRNA copies of target genes per 10^8 copies of 18S rRNA.

Statistical analysis. Statistical analyses were performed using GraphPad Prism Version 4.03 (GraphPad Software Inc., USA). Data were expressed as the mean ± standard error of mean (SEM). Statistical differences were analyzed using t-test. A p-value <0.05 was considered as significantly different.

Results

The effects of a high intracellular Zn^{2+} level on LNCaP cells proliferation. High intracellular Zn^{2+} was restored to the LNCaP prostate cancer cells as previously described (23). The LNCaP prostate cancer cell proliferation rate after the long-term culture in Zn^{2+} was examined by stimulating the cells to proliferate at week six post-initiation of the Zn^{2+} treatment (Fig. 1). The proliferation rate of cells cultured in 1 μg/ml Zn^{2+} was comparable to that of the non Zn^{2+}-treated cells (Fig. 2A). The proliferation rates for cells treated with supraphysiologic Zn^{2+} (10 μg/ml), however, were significantly lowered at 42.2±7.4%, 76.7±2.0% and 35.8±5.6% in comparison to the non Zn^{2+}-treated cells on days 3, 6 and 9, respectively (Fig. 2A). No significant growth differences were observed on day 12 (~7 weeks post-initiation of the treatment) between the supraphysiologic Zn^{2+}-supplemented cells (13.2±1.7%) and cells supplemented with only physiologic Zn^{2+} or without additional Zn^{2+}. In addition, the proliferation rate of cells supplemented with supraphysiologic Zn^{2+} was also significantly lower on days 3 and 6 (48.1±6.6% and 44.9±4.8%, respectively) when compared to that of the normal PNT2 prostate cells (Fig. 2A), suggesting that the

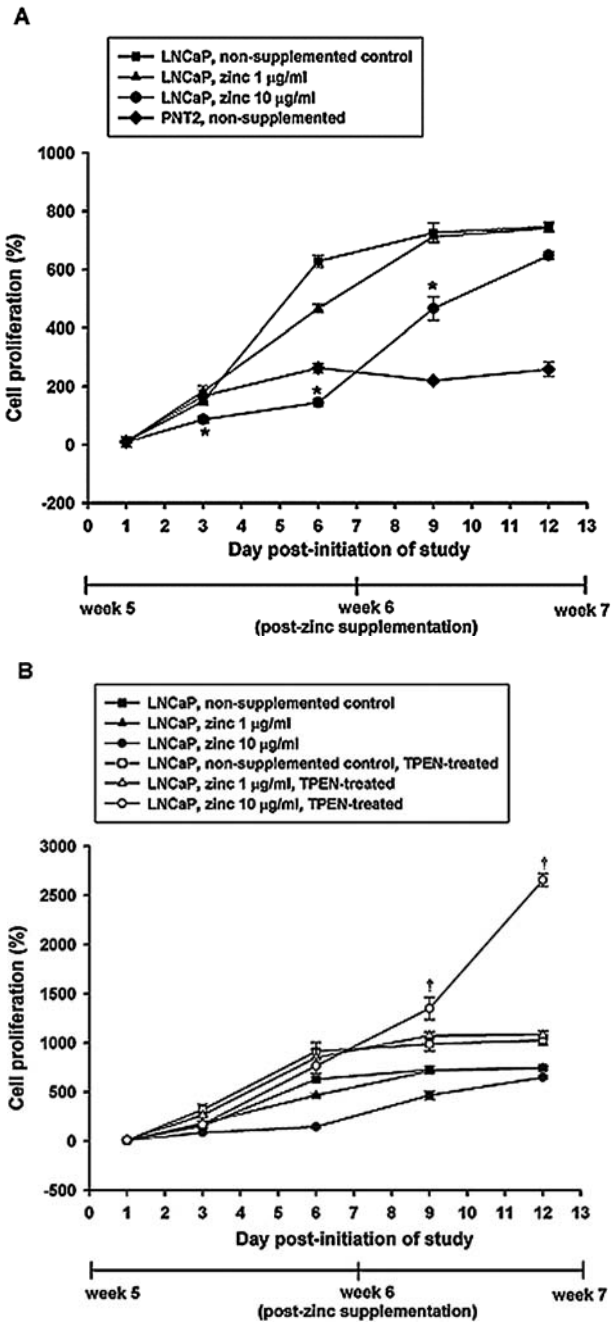

Figure 2. Effects of continuous supplementation with supraphysiologic Zn^{2+} concentration on LNCaP cell proliferation. Cell proliferation was determined over a period of 12 days and the percentage of viable cells was determined at selected intervals. The percentage of cell growth for cells cultured continuously in growth medium without additional Zn^{2+} (closed square), with only 1 μg/ml Zn^{2+} (closed triangle) and with 10 μg/ml Zn^{2+} (closed circle) were compared (A). The proliferation rates of cells when Zn^{2+} was chelated with TPEN from the control non-supplemented cells (open square), supplemented with only 1 μg/ml Zn^{2+} (open triangle) and with 10 μg/ml Zn^{2+} (open circle) were also determined (B). Lower bar indicates week post-initiation of the Zn^{2+} treatment. Asterisk indicates significantly different ($p<0.05$, t-test) when compared to LNCaP cells cultured without additional Zn^{2+} and † indicates significantly different ($p<0.05$, t-test) when compared to LNCaP cells supplemented with 10 μg/ml Zn^{2+} and then treated with TPEN.

high intracellular Zn^{2+} inhibited LNCaP cells proliferation. In contrast, the proliferation rates on day 9 and 12 were increased by 111.8±18.4% and 149.6±5.0%, respectively

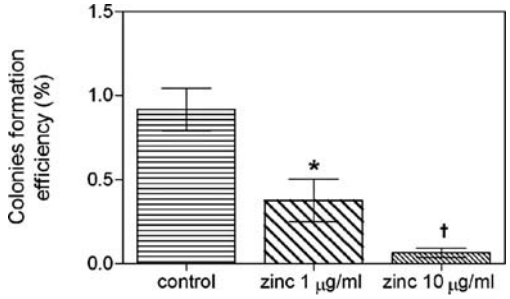

Figure 3. LNCaP cell anchorage-independent growth. LNCaP cells were cultured with and without Zn^{2+}-supplementation. Colony formation efficiency was determined using soft agar assay at week 5 post-initiation of the Zn^{2+} treatment. Approximately 5,000 cells from single cell suspension were seeded onto each well. The number of colonies formed 3 weeks post-seeding was counted and the average colonies formation efficiency of six replicates from each sample ± SEM is shown. *$p=0.0491$, †$p<0.0001$ (t-test) indicate significantly different in comparison to control non-supplemented cells.

in comparison to the PNT2 cells. These suggested that the high intracellular Zn^{2+} markedly reduced the LNCaP cell proliferation rate during the exponential phase following stimulation of cell growth but the growth rate accelerated by day 9 post-initiation of the cell proliferation. When Zn^{2+} was chelated from the supraphysiologic Zn^{2+}-supplemented LNCaP cells with TPEN, the cell proliferation rate increased dramatically by 427.2±55.1%, 189.6±24.5% and 309.9±10.3% on days 3, 6 and 9, respectively (Fig. 2B) in comparison to their respective non TPEN-treated counterparts, suggesting that high intracellular Zn^{2+} inhibited cell growth and the inhibition was removed when Zn^{2+} was chelated.

The effects of a high intracellular Zn^{2+} level on LNCaP prostate cancer cell colony formation efficiency. The effects of Zn^{2+} on the LNCaP cell anchorage-independent growth after 5 weeks of treatment were determined using the soft agar colony formation assay. Data from representative experiments (n=6) showed that the transformation frequency of the control non Zn^{2+}-supplemented LNCaP cells was 0.92±0.12%. The transformation frequencies for LNCaP cells supplemented with physiologic (1 μg/ml) and supraphysiologic (10 μg/ml) Zn^{2+} concentrations for 5 weeks were significantly reduced to 0.38±0.12% ($p<0.05$, t-test) and 0.06±0.02% ($p<0.0001$, t-test), respectively (Fig. 3). These findings suggested that the restoration of high intracellular Zn^{2+} transiently restricted LNCaP prostate cancer cell anchorage-independent growth after 5 weeks of treatment (Fig. 3).

The effects of a high intracellular Zn^{2+} level on LNCaP prostate cancer cell gene expression. The gene expression profile of LNCaP prostate cancer cells treated with supraphysiologic Zn^{2+} (10 μg/ml) for 5 weeks was examined using Illumina Human RefSeq-8 Sentrix Bead Chip 24,000 Gene Array (Illumina, USA). Data obtained were transformed and normalized to 50th percentile per chip and the median value per gene. Using a threshold factor of 1.5-fold change in signal intensity and Benjamini and Hochberg correction (FDR of 0.05), 161 zinc-upregulated genes were obtained without significantly downregulated genes (Fig. 4, Table II).

LNCaP prostate cancer cell genes responsive to supraphysiologic Zn^{2+}-treatment.

No.	GenBank accession no.	Gene	Fold-change	Corrected p-value
1	NM_001073	*Homo sapiens* UDP glycosyltransferase 2 family, polypeptide B11 (UGT2B11), mRNA	2.649	0.0295
2	NM_001074	*Homo sapiens* UDP glycosyltransferase 2 family, polypeptide B7 (UGT2B7), mRNA	2.496	0.0295
3	XM_378342	*Homo sapiens* hypothetical gene supported by BC003510; NM_002823	2.07	0.0295
4	XM_352588	*Homo sapiens* similar to 60S ribosomal protein L21 (LOC377296), mRNA	2	0.0295
5	NM_005950	*Homo sapiens* metallothionein 1G (MT1G), mRNA	1.986	0.0295
6	NM_006016	*Homo sapiens* CD164 antigen, sialomucin (CD164), mRNA	1.938	0.0295
7	XM_351136	*Homo sapiens* similar to ribosomal protein L7 (LOC374811), mRNA	1.929	0.0295
8	NM_012449	*Homo sapiens* six transmembrane epithelial antigen of the prostate (STEAP), mRNA	1.907	0.0295
9	XM_293276	*Homo sapiens* similar to Heat shock 27 kDa protein (HSP 27) (Stress-responsive protein 27) (SRP27) (Estrogen-regulated 24 kDa protein) (28 kDa heat shock protein) (LOC347348), mRNA	1.906	0.0295
10	NM_001436	*Homo sapiens* fibrillarin (FBL), mRNA	1.905	0.0295
11	XM_210334	*Homo sapiens* similar to 60S ribosomal protein L29 (Cell surface heparin binding protein HIP) (LOC284064), mRNA	1.902	0.0295
12	NM_005949	*Homo sapiens* metallothionein 1F (functional) (MT1F), mRNA	1.898	0.0295
13	NM_002354	*Homo sapiens* tumor-associated calcium signal transducer 1 (TACSTD1), mRNA	1.896	0.0295
14	NM_138369	*Homo sapiens* family with sequence similarity 44, member B (FAM44B), mRNA	1.892	0.0295
15	XM_377761	*Homo sapiens* similar to ribosomal protein L22 (LOC402100), mRNA	1.889	0.0295
16	XM_065828	*Homo sapiens* similar to 60S acidic ribosomal protein P1 (LOC130678), mRNA	1.872	0.0295
17	NM_004859	*Homo sapiens* clathrin, heavy polypeptide (Hc) (CLTC), mRNA	1.86	0.0295
18	NM_006135	*Homo sapiens* capping protein (actin filament) muscle Z-line, α 1 (CAPZA1), mRNA	1.841	0.0295
19	XM_291533	*Homo sapiens* similar to Transcription factor BTF3 (RNA polymerase B transcription factor 3) (LOC343363), mRNA	1.835	0.0295
20	NM_006743	*Homo sapiens* RNA binding motif protein 3 (RBM3), mRNA	1.822	0.0295
21	NM_020368	*Homo sapiens* disrupter of silencing 10 (SAS10), mRNA	1.818	0.0295
22	XM_041018	*Homo sapiens* KIAA0367 protein (KIAA0367), mRNA	1.805	0.0295
23	NM_145266	*Homo sapiens* nudix (nucleoside diphosphate linked moiety X) -type motif 8 (NUDT8), mRNA	1.804	0.0295
24	NM_005063	*Homo sapiens* stearoyl-CoA desaturase δ-9-desaturase) (SCD), mRNA	1.799	0.0295
25	XM_060535	*Homo sapiens* similar to ribosomal protein L18a; 60S ribosomal protein L18a (LOC127545), mRNA	1.785	0.0295
26	XM_292012	*Homo sapiens* similar to Polyadenylate-binding protein 1 (Poly(A)-binding protein 1) (PABP 1) (LOC341315), mRNA	1.78	0.0295
27	XM_372315	*Homo sapiens* similar to 60S ribosomal protein L12 (LOC389974), mRNA	1.766	0.0295
28	NM_001077	*Homo sapiens* UDP glycosyltransferase 2 family, polypeptide B17 (UGT2B17), mRNA	1.76	0.0295
29	NM_031263	*Homo sapiens* heterogeneous nuclear ribonucleoprotein K (HNRPK), transcript variant 3, mRNA	1.76	0.0295
30	NM_012248	*Homo sapiens* selenophosphate synthetase 2 (SEPHS2), mRNA	1.759	0.0295
31	NM_002439	*Homo sapiens* mutS homolog 3 (*E. coli*) (MSH3), mRNA	1.756	0.0323
32	XM_378321	*Homo sapiens* hypothetical gene supported by AK096370 (LOC399972), mRNA	1.754	0.0295
33	XM_352441	*Homo sapiens* similar to Ubiquinol-cytochrome C reductase complex 11 kDa protein, mitochondrial precursor (Mitochondrial hinge protein) (Cytochrome C1, nonheme 11 kDa protein) (Complex III subunit VIII)	1.751	0.031

Table II. Continued.

No.	GenBank accession no.	Gene	Fold-change	Corrected p-value
34	NM_181843	*Homo sapiens* oxysterol binding protein-like 8 (OSBPL8), mRNA	1.751	0.0295
35	NM_004265	*Homo sapiens* fatty acid desaturase 2 (FADS2), mRNA	1.741	0.0295
36	XM_377480	*Homo sapiens* similar to 60S ribosomal protein L17 (L23) (Amino acid starvation-induced protein) (ASI) (LOC401886), mRNA	1.74	0.0295
37	NM_002822	*Homo sapiens* PTK9 protein tyrosine kinase 9 (PTK9), transcript variant 1, mRNA	1.738	0.0295
38	NM_001212	*Homo sapiens* complement component 1, q subcomponent binding protein (C1QBP), nuclear gene encoding mitochondrial protein, mRNA	1.734	0.0295
39	NM_004060	*Homo sapiens* cyclin G1 (CCNG1), transcript variant 1, mRNA	1.73	0.0295
40	XM_292526	*Homo sapiens* similar to peptidylprolyl isomerase A (cyclophilin A) (LOC342405), mRNA	1.728	0.0295
41	NM_021218	*Homo sapiens* chromosome 9 open reading frame 80 (C9orf80), mRNA	1.726	0.0323
42	NM_175573	*Homo sapiens* adhesion regulating molecule 1 (ADRM1), transcript variant 2, mRNA	1.725	0.0298
43	NM_004685	*Homo sapiens* myotubularin related protein 6 (MTMR6), mRNA	1.721	0.0295
44	NM_003506	*Homo sapiens* frizzled homolog 6 (*Drosophila*) (FZD6), mRNA	1.717	0.0295
45	NM_000055	*Homo sapiens* butyrylcholinesterase (BCHE), mRNA	1.706	0.0295
46	NM_014016	*Homo sapiens* SAC1 suppressor of actin mutations 1-like (yeast) (SACM1L), mRNA	1.706	0.0295
47	NM_007363	*Homo sapiens* non-POU domain containing, octamer-binding (NONO), mRNA	1.687	0.0295
48	NM_004593	*Homo sapiens* splicing factor, arginine/serine-rich 10 (transformer 2 homolog, *Drosophila*) (SFRS10), mRNA	1.685	0.0295
49	NM_017932	*Homo sapiens* hypothetical protein FLJ20700 (FLJ20700), mRNA	1.683	0.0323
50	XM_377516	*Homo sapiens* similar to ribosomal protein L28; 60S ribosomal protein L28 (LOC401900), mRNA	1.676	0.0295
51	NM_006079	*Homo sapiens* Cbp/p300-interacting transactivator, with Glu/Asp-rich carboxy-terminal domain, 2 (CITED2), mRNA	1.675	0.0298
52	NM_022874	*Homo sapiens* survival of motor neuron 1, telomeric (SMN1), transcript variant b, mRNA	1.675	0.0295
53	NM_000441	*Homo sapiens* solute carrier family 26, member 4 (SLC26A4), mRNA	1.674	0.0295
54	NR_003608	*Homo sapiens* α tubulin-like (MGC16703), mRNA	1.674	0.0298
55	NM_145266	*Homo sapiens* NudC domain containing 2 (NUDCD2), mRNA	1.67	0.0295
56	NM_173669	*Homo sapiens* hypothetical protein FLJ34047 (FLJ34047), mRNA	1.67	0.0295
57	NM_005782	*Homo sapiens* THO complex 4 (THOC4), mRNA	1.67	0.0295
58	NM_000687	*Homo sapiens* S-adenosylhomocysteine hydrolase (AHCY), mRNA	1.669	0.0295
59	NM_030779	*Homo sapiens* potassium voltage-gated channel, subfamily H (eag-related), member 6 (KCNH6), transcript variant 1, mRNA	1.666	0.0295
60	XM_352086	*Homo sapiens* similar to Small nuclear ribonucleoprotein Sm D2 (snRNP core protein D2) (Sm-D2) (LOC376142), mRNA	1.663	0.0295
61	NM_014291	*Homo sapiens* glycine C-acetyltransferase (2-amino-3-ketobutyrate coenzyme A ligase) (GCAT), nuclear gene encoding mitochondrial protein, mRNA	1.663	0.0295
62	NM_201453	*Homo sapiens* COBW domain containing 3 (CBWD3), mRNA	1.659	0.0295
63	NM_003969	*Homo sapiens* ubiquitin-conjugating enzyme E2M (UBC12 homolog, yeast) (UBE2M), mRNA	1.658	0.0295
64	NM_017900	*Homo sapiens* aurora-A kinase interacting protein (AKIP), mRNA	1.657	0.0295
65	NM_001527	*Homo sapiens* histone deacetylase 2 (HDAC2), mRNA	1.657	0.0295
66	XM_352331	*Homo sapiens* similar to dJ612B18.1 (similar to 40S ribosomal protein) (LOC376679), mRNA	1.655	0.0295
67	NM_014501	*Homo sapiens* ubiquitin-conjugating enzyme E2S (UBE2S), mRNA	1.653	0.0295
68	NM_144682	*Homo sapiens* hypothetical protein FLJ31952 (FLJ31952), mRNA	1.653	0.0295

 Continued.

No.	GenBank accession no.	Gene	Fold-change	Corrected p-value
69	NM_080821	*Homo sapiens* chromosome 20 open reading frame 108 (C20orf108), mRNA	1.652	0.0295
70	NM_032026	*Homo sapiens* TatD DNase domain containing 1 (TATDN1), mRNA	1.652	0.0295
71	NM_022098	*Homo sapiens* X-prolyl aminopeptidase (aminopeptidase P) 3, putative (XPNPEP3), mRNA	1.643	0.0295
72	NM_003952	*Homo sapiens* ribosomal protein S6 kinase, 70 kDa, polypeptide 2 (RPS6KB2), mRNA	1.642	0.0295
73	XM_063202	*Homo sapiens* similar to 60S ribosomal protein L23a (LOC122585), mRNA	1.641	0.0298
74	NM_000982	*Homo sapiens* ribosomal protein L21 (RPL21), mRNA	1.639	0.0295
75	NM_203448	*Homo sapiens* hypothetical protein MGC21881 (MGC21881), mRNA	1.638	0.0295
76	NM_032194	*Homo sapiens* brix domain containing 1 (BXDC1), mRNA	1.635	0.0295
77	NM_000745	*Homo sapiens* cholinergic receptor, nicotinic, α polypeptide 5 (CHRNA5), mRNA	1.634	0.0295
78	NM_016097	*Homo sapiens* immediate early response 3 interacting protein 1(IER3IP1), mRNA	1.634	0.0295
79	NM_006948	*Homo sapiens* stress 70 protein chaperone, microsome-associated, 60 kDa (STCH), mRNA	1.633	0.0306
80	NM_016126	*Homo sapiens* chromosome 1 open reading frame 41 (C1orf41), mRNA	1.632	0.0295
81	NM_032478	*Homo sapiens* mitochondrial ribosomal protein L38 (MRPL38), nuclear gene encoding mitochondrial protein, mRNA	1.628	0.0295
82	NM_016221	*Homo sapiens* dynactin 4 (p62) (DCTN4), mRNA	1.625	0.0298
83	NM_025065	*Homo sapiens* brix domain containing 5 (BXDC5), mRNA	1.62	0.0295
84	NM_005642	*Homo sapiens* TAF7 RNA polymerase II, TATA box binding protein (TBP)-associated factor, 55 kDa (TAF7), mRNA	1.62	0.0298
85	XM_350967	*Homo sapiens* similar to 40S ribosomal protein S8 (LOC374596), mRNA	1.619	0.0397
86	NM_014820	*Homo sapiens* translocase of outer mitochondrial membrane 70 homolog A (yeast) (TOMM70A), mRNA	1.617	0.0298
87	XM_380042	*Homo sapiens* similar to 60S ribosomal protein L15 (LOC402694), mRNA	1.615	0.0447
88	NM_003143	*Homo sapiens* single-stranded DNA binding protein 1 (SSBP1), mRNA	1.613	0.0295
89	NM_004772	*Homo sapiens* chromosome 5 open reading frame 13 (C5orf13), mRNA	1.612	0.0295
90	NM_006756	*Homo sapiens* transcription elongation factor A (SII), 1 (TCEA1), transcript variant 1, mRNA	1.61	0.0295
91	NM_177985	*Homo sapiens* ADP-ribosylation factor-like 5 (ARL5), transcript variant 2, mRNA	1.606	0.0295
92	NM_173494	*Homo sapiens* chromosome X open reading frame 41 (CXorf41), mRNA	1.602	0.0295
93	NM_001064	*Homo sapiens* transketolase (Wernicke-Korsakoff syndrome) (TKT), mRNA	1.601	0.0295
94	NM_181054	*Homo sapiens* hypoxia-inducible factor 1, α subunit (basic helix-loop-helix transcription factor) (HIF1A), transcript variant 2, mRNA	1.601	0.0298
95	NM_002154	*Homo sapiens* heat shock 70 kDa protein 4 (HSPA4), transcript variant 1, mRNA	1.596	0.0295
96	NM_003634	*Homo sapiens* nipsnap homolog 1 (*C. elegans*) (NIPSNAP1), mRNA	1.595	0.0295
97	NM_203373	*Homo sapiens*s F-box and leucine-rich repeat protein 22 (FBXL22), mRNA	1.595	0.0295
98	NM_003666	*Homo sapiens* basic leucine zipper nuclear factor 1 (JEM-1) (BLZF1), mRNA	1.594	0.0298
99	NM_023009	*Homo sapiens* MARCKS-like protein (MLP), mRNA	1.594	0.0295
100	NM_032351	*Homo sapiens* mitochondrial ribosomal protein L45 (MRPL45), nuclear gene encoding mitochondrial protein, mRNA	1.593	0.0295
101	NM_152678	*Homo sapiens* family with sequence similarity 116, member A (FAM116A), mRNA	1.591	0.0298
102	NM_182763	*Homo sapiens* myeloid cell leukemia sequence 1 (BCL2-related) (MCL1), transcript variant 2, mRNA	1.586	0.0306
103	NM_003671	*Homo sapiens* CDC14 cell division cycle 14 homolog B (*S. cerevisiae*) (CDC14B), transcript variant 1, mRNA	1.586	0.0298

Table II. Continued.

No.	GenBank accession no.	Gene	Fold-change	Corrected p-value
104	NM_054026	*Homo sapiens* CCR4-NOT transcription complex, subunit 7 (CNOT7), transcript variant 2, mRNA	1.584	0.0295
105	NM_198264	*Homo sapiens* chromosome 1 open reading frame 2 (C1orf2), transcript variant 2, mRNA	1.582	0.0295
106	NM_031459	*Homo sapiens* sestrin 2 (SESN2), mRNA	1.582	0.031
107	NM_018467	*Homo sapiens* uncharacterized hematopoietic stem/progenitor cells protein MDS032 (MDS032), mRNA	1.579	0.031
108	NM_017547	*Homo sapiens* FAD-dependent oxidoreductase domain containing 1 (FOXRED1), mRNA	1.577	0.0298
109	NM_033630	*Homo sapiens* SCAN domain containing 1 (SCAND1) transcript variant 2, mRNA	1.577	0.0295
110	NM_032710	*Homo sapiens* hypothetical protein MGC13053 (MGC13053), mRNA	1.576	0.0381
111	XM_370684	*Homo sapiens* similar to Elongation factor 1-α 1 (EF-1-α-1) (Elongation factor 1 A-1) (eEF1A-1) (Elongation factor Tu) (EF-Tu) (LOC387845), mRNA	1.575	0.0295
112	XM_351078	*Homo sapiens* similar to protein 40 kDa (LOC374744), mRNA	1.574	0.0295
113	NM_000994	*Homo sapiens* ribosomal protein L32 (RPL32), mRNA	1.573	0.0295
114	NM_025030	*Homo sapiens* hypothetical protein FLJ20972 (FLJ20972), mRNA	1.573	0.0295
115	NM_013410	*Homo sapiens* adenylate kinase 3 (AK3), mRNA	1.572	0.0295
116	XM_352732	*Homo sapiens* similar to L21 ribosomal protein (LOC377653), mRNA	1.572	0.0298
117	NM_016141	*Homo sapiens* dynein, cytoplasmic, light intermediate polypeptide 1 (DNCLI1), mRNA	1.57	0.0295
118	NM_014056	*Homo sapiens* likely ortholog of mouse hypoxia induced gene 1 (HIG1), mRNA	1.566	0.0295
119	XM_209959	*Homo sapiens* similar to chromosome 7 open reading frame 17 protein; 16.7 kDa protein (LOC286224), mRNA	1.565	0.0309
120	NM_015431	*Homo sapiens* BIA2 (BIA2), mRNA	1.563	0.0298
121	NM_031901	*Homo sapiens* mitochondrial ribosomal protein S21 (MRPS21), nuclear gene encoding mitochondrial protein, transcript variant 1, mRNA	1.562	0.0295
122	NM_006835	*Homo sapiens* cyclin I (CCNI), mRNA	1.561	0.0295
123	NM_001949	*Homo sapiens* E2F transcription factor 3 (E2F3), mRNA	1.56	0.0295
124	NM_003440	*Homo sapiens* zinc finger protein 140 (ZNF140), mRNA	1.559	0.0295
125	XM_371658	*Homo sapiens* similar to laminin receptor 1 (ribosomal protein SA); P40-3, functional; P40-8, functional; laminin receptor 1 (67 kDa, ribosomal protein SA) (LOC389141), mRNA	1.553	0.0295
126	NM_001660	*Homo sapiens* ADP-ribosylation factor 4 (ARF4), mRNA	1.552	0.0295
127	NM_133509	*Homo sapiens* RAD51-like 1 (*S. cerevisiae*) (RAD51L1), transcript variant 3, mRNA	1.552	0.0298
128	NM_004768	*Homo sapiens* splicing factor, arginine/serine-rich 11 (SFRS11), mRNA	1.549	0.0295
129	NM_022483	*Homo sapiens* hypothetical protein FLJ21657 (FLJ21657), mRNA	1.547	0.0295
130	NM_002395	*Homo sapiens* malic enzyme 1, NADP(+)-dependent, cytosolic (ME1), mRNA	1.547	0.0295
131	NM_004986	*Homo sapiens* kinectin 1 (kinesin receptor) (KTN1), mRNA	1.545	0.0295
132	XM_352485	*Homo sapiens* similar to ATP synthase α chain, mitochondrial precursor (LOC376965), mRNA	1.545	0.0295
133	NM_020387	*Homo sapiens* RAB25, member RAS oncogene family (RAB25), mRNA	1.537	0.0295
134	NM_024040	*Homo sapiens* CUE domain containing 2 (CUEDC2), mRNA	1.537	0.0295
135	NM_002156	*Homo sapiens* heat shock 60 kDa protein 1 (chaperonin) (HSPD1), nuclear gene encoding mitochondrial protein, transcript variant 1, mRNA	1.532	0.0295
136	NM_178812	*Homo sapiens* metadherin (MTDH), mRNA	1.532	0.0295
137	NM_005367	*Homo sapiens* melanoma antigen, family A, 12 (MAGEA12), mRNA	1.531	0.0295

Continued.

No.	GenBank accession no.	Gene	Fold-change	Corrected p-value
138	NM_001562	*Homo sapiens* interleukin 18 (interferon-γ-inducing factor) (IL18), mRNA	1.53	0.04
139	NM_003352	*Homo sapiens* SMT3 suppressor of mif two 3 homolog 1 (yeast) (SUMO1), mRNA	1.529	0.0341
140	NM_016308	*Homo sapiens* cytidine monophosphate (UMP-CMP) kinase 1, cytosolic (CMPK1), mRNA	1.526	0.0295
141	XM_352661	*Homo sapiens* similar to dynein, cytoplasmic, light peptide (LOC377527), mRNA	1.526	0.0295
142	NM_001029	*Homo sapiens* ribosomal protein S26 (RPS26), mRNA	1.526	0.0295
143	NM_003746	*Homo sapiens* dynein, cytoplasmic, light polypeptide 1 (DNCL1), mRNA	1.524	0.0295
144	NM_006457	*Homo sapiens* PDZ and LIM domain 5 (PDLIM5), mRNA	1.523	0.0306
145	NM_005274	*Homo sapiens* guanine nucleotide binding protein G protein), -γ 5 (GNG5), mRNA	1.523	0.0295
146	NM_183003	*Homo sapiens* cytochrome c oxidase subunit VIIa polypeptide 3 (liver) (COX7A3), mRNA	1.522	0.0485
147	NM_014045	*Homo sapiens* low density lipoprotein receptor-related protein 10 (LRP10), mRNA	1.522	0.0295
148	NM_007265	*Homo sapiens* ecdysoneless homolog (*Drosophila*) (ECD), mRNA	1.52	0.0298
149	NM_198853	*Homo sapiens* tripartite motif-containing 50C (TRIM50C), mRNA	1.514	0.0295
150	NM_000791	*Homo sapiens* dihydrofolate reductase (DHFR), mRNA	1.513	0.0373
151	NM_020841	*Homo sapiens* p53 target zinc finger protein (WIG1), transcript variant 2, mRNA	1.513	0.0298
152	NM_032796	*Homo sapiens* synapse associated protein 1, SAP47 homolog (*Drosophila*) (SYAP1), mRNA	1.513	0.0298
153	NM_006763	*Homo sapiens* BTG family, member 2 (BTG2), mRNA	1.511	0.0295
154	XM_293026	*Homo sapiens* similar to UNR-interacting protein (WD-40 repeat protein PT-WD) (MAP activator with WD repeats) (LOC344382), mRNA	1.508	0.0463
155	NM_017636	*Homo sapiens* transient receptor potential cation channel, subfamily M, member 4 (TRPM4), mRNA	1.508	0.0463
156	NM_014637	*Homo sapiens* mitochondrial fission regulator 1 (MTFR1), nuclear gene encoding mitochondrial protein, mRNA	1.505	0.0295
157	NM_013402	*Homo sapiens* fatty acid desaturase 1 (FADS1), mRNA	1.502	0.0381
158	NM_015251	*Homo sapiens* KIAA0431 protein (KIAA0431), mRNA	1.501	0.0401
159	NM_183352	*Homo sapiens* SEC13 homolog (*S. cerevisiae*) (SEC13), transcript variant 1, mRNA	1.501	0.0357
160	NM_003029	*Homo sapiens* SHC (Src homology 2 domain containing) transforming protein 1 (SHC1), mRNA	1.501	0.0295
161	NM_016535	*Homo sapiens* zinc finger protein 581 (ZNF581), mRNA	1.501	0.0295

The mRNA expressions of selected genes from the list of genes that were highly responsive to the Zn^{2+} treatment were further quantified using quantitative real-time RT-PCR (RT-qPCR). Of the 9 selected genes, 4 genes showed comparable mRNA expression fold changes to those found in microarray analysis while the other 5 genes had even higher fold changes when compared to those identified from the microarray analysis (Fig. 5). At least 12 different functional gene groups were obtained from the 161 genes found responsive to high intracellular Zn^{2+} when clustered based on biological process categories of the Gene Ontology Consortium (Fig. 6) using the web-based annotation program NMC Annotation Tool (26). These groups consist of genes that encode for proteins involved in translation (10.6%), cell proliferation/cell death/cell cycle regulation (7.6%), signal transduction (8.1%), metabolism (8.6%), transcription (8.6%), ion/protein transport

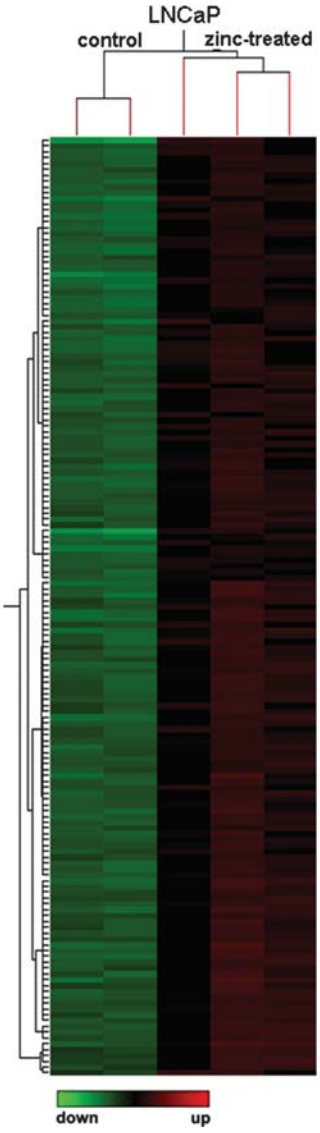

Figure 4. Hierarchical clustering of genes based on responsiveness to Zn^{2+}. LNCaP cells cultured in growth medium without Zn^{2+} supplementation or with 10 μg/ml Zn^{2+} are indicated by columns and the gene specific probes are indicated by rows. A total of 161 significant ($p<0.05$, t-test) gene specific probe signals were analyzed. Total cellular RNA of the Zn^{2+}-treated cells at the end of passage 5 (week 5) was used for preparation of target RNA for hybridization.

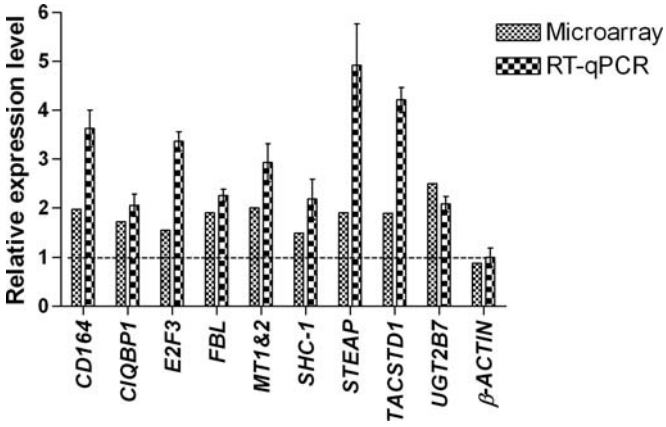

Figure 5. Gene expression in LNCaP prostate cancer cells in response to prolonged treatment with supraphysiologic Zn^{2+}. The mRNA expression (>1.5-fold increase) changes identified by microarray analysis were evaluated using quantitative RT-PCR (RT-qPCR). The mRNA copies were normalized to 18S rRNA and then plotted as ratio of the corresponding levels in the Zn^{2+}-treated cells in comparison to the non Zn^{2+}-supplemented cells (mean ± SEM). The average of fold increase of all the selected genes was 1-fold over that of the non Zn^{2+} treated LNCaP cells. The values were obtained from at least three independent amplifications of triplicates.

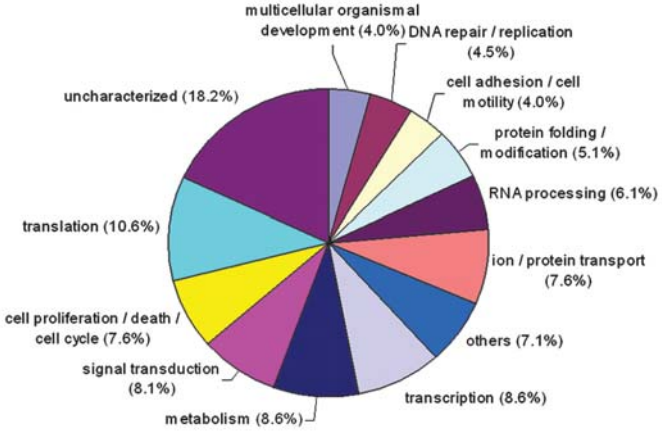

Figure 6. Functional grouping of genes that were upregulated in LNCaP cells following restoration of high intracellular Zn^{2+}.

(7.6%), RNA processing (6.1%), protein folding/modification (5.1%), cell adhesion/cell motility (4.0%), DNA repair/DNA replication (4.5%) and multicellular organismal development (4.0%). Several genes that are involved in various biological processes such as immune responses, secretion, excretion, endocytosis and sensory perception of sound were grouped under 'other' category (7.1%) and a larger fraction of the genes (18.2%), comprised of hypothetical genes or genes with unknown function were grouped under 'uncharacterized' category.

The microarray analysis revealed several genes associated with cell growth inhibition, DNA damage/repair, oxidative stress and decreased tumor colony formation abilities were affected by the high intracellular Zn^{2+} treatment of the LNCaP cells. These included *BTG2* (28), *CCNG1* (29), *KIAA0367/BMCC1* (30), *C1QBP/HABP1/gC1qR* (31), *HSPD1* (32), *SESN2* (33), *MLP* (34), *RBM3* (35), *MT-1F* (36) and *SHC-1* (37) that negatively regulate cell growth. Whereas, *RAD51L1*, *MSH3* (38), *ATMIN* (39) and *NONO* (40) were upregulated usually in response to DNA damage/repair and *ME1* (41), was upregulated in response to oxidative stress. *MT-1F* (42) and *WIG1/ZMAT3* (43) found upregulated were usually associated to a decrease in tumor colony formation efficiency similar to results obtained when the LNCaP cells were treated with supraphysiologic Zn^{2+} at 5 weeks post-treatment (Table III). Approximately 16.1% of the up-regulated genes, however, were genes commonly found over-expressed in malignant tissues/cells and those that promote cell proliferation, adhesion and migration (Table III). These included *CD164* (44), *FASN* (45), *FAD* (46), *NONO/Nmt55* (47), *CCNG1* (48), *TACSTD1* (49), *ADRM1* (50), *HIF1A* (51), *MAGE A12* (52), *RPL4*, *RPL23a* (53), *CITED2* (54), *ARL5* (55) and *FBL* (56). Some of these genes were also

Selected LNCaP cell genes that responded to the high intracellular Zn^{2+} treatment.

Gene symbol	Cellular effects
AHCY, *BTG2*, *CCNG1*, *C1QBP1*, *HSPD1*, *MLP*, *KIAA0367/BMCC1*, *MT-1F*, *RBM3*, *SESN2*, *SHC-1*	Cell growth inhibition, apoptosis
ATMIN, *MSH3*, *MT-1F*, *NONO*, *SESN2*, *RAD51L1*, *ME1*	DNA damage/repair, oxidative stress, hypoxia
MT-1F, *WIG1/ZMAT3*	Decrease tumour colonies formation capability
SCD, *CD164*[a], *CITED2*, *E2F3*[a], *STEAP1*[a], *ADRM1*	Metastasis and invasion
AHR, *E2F3*, *JEM-1/BLZF1*, *SCD*, *SHC-1*, *TKT*	Cell proliferation
ADRM1, *CCNG1*, *FAD2*, *FBL*, *NONO*, *RPL4*, *RPL23a*, *TACSTD1*[a]	Overexpressed in cancers: prostate cancer
E2F3 and *STEAP1*	Prostate, bladder, colon, ovarian cancer, Ewing sarcoma
ARL5, *KTN1* and *MT-1F*	Liver cancer
RPL29	Colon cancer
AHCY	Ovarian cancer
HIF1A	Rectal cancer
MAGE A12	Oral squamous carcinoma
HIG1, FBL[a]	Cervical squamous cell, hepatocellular carcinoma

[a]Genes selected for short-term Zn^{2+}-treatment and RT-qPCR analysis in LNCaP and PNT2 cells.

Table IV. Comparison of mRNA expression levels between LNCaP prostate cancer and PNT2 normal cell genes at 72 h post Zn^{2+}-treatment.

	LNCaP[a]		PNT2[a]	
Genes	Control (Untreated)	Zn^{2+}-treated (10 μg/ml)	Control (Untreated)	Zn^{2+}-treated (10 μg/ml)
CD164	+ +	+ + +	+ +	+ + +
FBL	+ + +	+ + + +	+	+ +
TACSTD1	+ + +	+ + + +	+ + +	+ + + +
E2F3	+ + +	+ + + +	+ + +	+ + +
STEAP1	+ + +	+ + +	+	+

[a]mRNA copies per 10^8 copies of 18S rRNA; +, <$5.0x10^7$ copies; + +, $5.0x10^7$-$1.0x10^8$ copies; + + +, $1.0x10^8$-$5.0x10^8$ copies; + + + +, >$5.0x10^8$ copies.

previously reported to be overexpressed in prostate cancer tissues (44-47,49,50,53,57-59).

The effects of short-term Zn^{2+} treatments on LNCaP and PNT2 cell gene expression. Five genes identified as highly responsive (>1.7-fold, with exception of E2F3 gene at ~1.5 fold) to supraphysiologic Zn^{2+} concentration from the 161 Zn^{2+}-responsive genes were selected for further examination in LNCaP prostate cancer cells and PNT2 prostate normal cells. PNT2 and LNCaP cells were treated with 10 μg/ml Zn^{2+} and the mRNA expression levels at intervals up to 72 h were quantified by quantitative reverse transcriptase PCR (RT-qPCR). Results obtained for LNCaP cells treated with Zn^{2+} (10 μg/ml) for 5 weeks were included for comparison. Comparative transcription studies of *CD164*, *E2F3*, *FBL*, *STEAP1* and *TACSTD1* genes showed a time-dependent increase in mRNA expression levels of these genes in the Zn^{2+}-treated LNCaP cells beginning at 16 h post-treatment (Fig. 7). The mRNA expression levels of these genes in the non Zn^{2+}-treated cells harvested at 72 h and cells treated with 100 μM *N*, *N*, *N*', *N*'-tetrakis(2-pyridylmethyl)ethylenediamine (TPEN) to chelate Zn^{2+} remained lower than the Zn^{2+}-treated cells. At 16 h post-treatment, the mRNA levels of *CD164*, *FBL* and *TACSTD1* genes of the Zn^{2+}-treated LNCaP cells were 2.2±0.3-fold, 4.5±0.7-fold and 2.7±0.6-fold, respectively, higher than the non Zn^{2+}-treated LNCaP cells (Fig. 7A, C and E; $p<0.01$, t-test). The mid logarithmic increase in the mRNA expression for *CD164*, *FBL* and *TACSTD1* genes were observed at ~18 h post-treatment (Fig. 7). At 72 h post-treatment, the mRNA expression of *CD164*, *FBL* and *TACSTD1* had increased by 3.5±0.4-fold ($p<0.01$, t-test), 5.6±0.6-fold ($p<0.001$, t-test) and 5.1±0.5-fold ($p<0.001$, t-test) when compared to the non Zn^{2+}-treated LNCaP cells (Table IV). On the other hand, the mid logarithmic increase in the mRNA expression of *E2F3* and *STEAP1* genes was at ~36 h post-treatment suggesting a delay in response to Zn^{2+} by these genes. At 48 h post-treatment, the mRNA expression levels of *E2F3* and *STEAP1* of the Zn^{2+}-treated LNCaP cells were 3.03±0.7-fold ($p=0.046$, t-test) and 2.0±0.3-fold ($p<0.001$, t-test), respectively, higher than the non Zn^{2+}-treated LNCaP cells and remained almost unchanged at 72 h post-treatment (3.3±0.3-fold and 3.1±0.3-fold, respectively) (Fig. 7B and D; Table IV). At 5 weeks post-treatment, the mRNA expression of *CD164*, *FBL*, *TACSTD1*, *E2F3* and *STEAP1* genes remained high, at 3.6±0.4-fold, 2.0±0.1-fold, 4.2±0.3-fold, 3.4±0.2-fold and

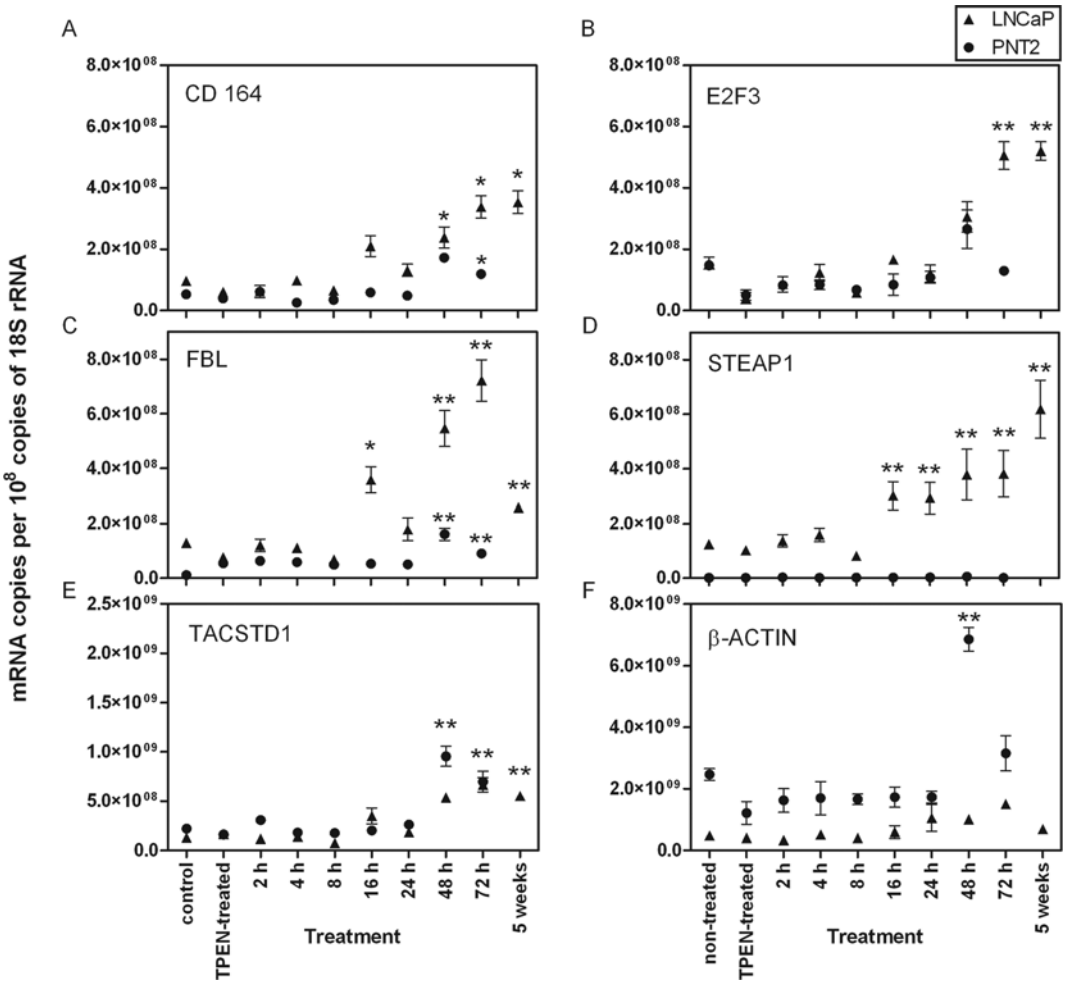

Figure 7. Expression profiles of LNCaP prostate cancer and PNT2 normal cells genes responding to the short- and long-term exposure to Zn^{2+}. LNCaP and PNT2 cells were treated with 10 μg/ml Zn^{2+} for 2, 4, 8, 16, 24, 48 and 72 h. Control untreated cells and cells treated with 100 μM *N*, *N*, *N*', *N*'-tetrakis (2-pyridylmethyl)ethylenediamine (TPEN) to chelate Zn^{2+} were incubated in parallel up to 72 h. *CD164*, CD164 sialomucin (A); *E2F3*, E2F transcription factor 3 (B); *FBL*, fibrillarin (C); *STEAP1*, six-transmembrane epithelial antigen of the prostate 1 (D); *TACSTD1*, tumor-associated calcium signal transducer 1 (E); and ß-actin (F). $^{*}p<0.01$, $^{**}p<0.001$ (t-test).

4.9±0.9-fold, respectively, in comparison to the non Zn^{2+}-treated LNCaP (Fig. 7).

The mRNA expression of *CD164*, *FBL* and *TACSTD1* in the Zn^{2+}-treated PNT2 increased only beginning at 48 h post-treatment and this was in contrast to 16 h in the LNCaP cells (Fig. 7). The mRNA levels of *CD164*, *FBL* and *TACSTD1* increased by 3.3±0.1-fold, 13.5±1.9-fold and 4.4±0.5-fold higher than the non Zn^{2+}-treated PNT2 cells (Fig. 7A, C and E). At 72 h post-treatment, the mRNA levels of *CD164*, *FBL* and *TACSTD1* increased by 2.2±0.2-fold, 7.6±1.0-fold and 3.2±0.5-fold higher than theZn^{2+}-treated PNT2 cells (Fig. 7A, C and E). The mRNA levels of the house-keeping gene, ß-actin, also increased by 2.8±0.2-fold and 1.3±0.2-fold at 48 and 72 h post-treatment, respectively, in the non Zn^{2+}-treated PNT2 cells (Fig. 7F). The levels of ß-actin mRNA were otherwise unchanged at other time points in both the Zn^{2+}-treated LNCaP and PNT2 cells. The slight increase in ß-actin mRNA was not unexpected as 18S rRNA was used for normalization of the data in the study and it has its shortcomings (60,61).

The RT-qPCR results from the study showed that the cell growth promoting genes *CD164*, *FBL* and *TACSTD1* were responsive to the high intracellular Zn^{2+} treatment in both PNT2 prostate normal and LNCaP prostate cancer cells (Table IV). *FBL* and *STEAP1*, however, were constitutively higher in LNCaP cells in comparison to the PNT2 cells. *FBL* and STEAP1 were especially very high in LNCaP cells. The *E2F3* gene responded to the Zn^{2+} treatment in LNCaP, but not PNT2 cells. STEAP1 expression was not responsive to the Zn^{2+} treatment in either cells and perhaps reflects the absence of pathways involving Zn^{2+} in the regulation of *STEAP1* expression. Collectively these findings suggested that among the genes investigated only *CD164*, *FBL* and *TACSTD1* were responsive to changes in the intracellular zinc concentration in prostate normal as well as cancer cells and despite the constitutively high level of expression in LNCaP cells, *FBL* gene can still be superinduced in the presence of supraphysiologic Zn^{2+}.

Discussion

The normal prostate gland has a high level of Zn^{2+}. Its role in prostate cell growth and gene expression, however, remains unclear. It is known that the Zn^{2+} level is significantly reduced

e malignancies. The present study investigates the restoring high intracellular Zn^{2+} to LNCaP prostate cancer cells and its effects on cell growth and specific gene expression. An environment of high intracellular Zn^{2+} level is restored to the LNCaP prostate cancer cells by continuously culturing the cells over a 5-week period in growth media supplemented with physiologic (1 μg/ml) and supraphysiologic (10 μg/ml) concentrations of Zn^{2+}. The treatment successfully increased the intracellular Zn^{2+} concentration and the number of zincosomes, a Zn^{2+}-specific vesicle (23). Results from our microarray study, further suggest that the increase in intracellular Zn^{2+} level is also reflected by the increase in mRNA expressions of MT-1G and MT-1F which are radical scavengers that chelate and sequester excessive metal ions (11). The Zn^{2+} treatment, however, did not result in significant changes in the mRNA expression of Zn^{2+} transporters, hZIP-1 and ZnT1, which is in agreement with an earlier report (62) suggesting that regulation of these transporter gene expressions is not directly regulated by the intracellular Zn^{2+} level.

It is shown in the present study that cells treated with supraphysiologic Zn^{2+} exhibited reduced cell proliferation rate at the exponential point only. The inhibition is transient as the cell proliferation rate and anchorage-independent growth later attained the levels comparable to that of untreated cells. These results are incongruent with an earlier study that shows that there is no induction of senescence or apoptosis in the Zn^{2+}-treated cell cultures (24). It also suggests that somehow the initial inhibitory effects of Zn^{2+} on LNCaP cell proliferation is reversed in the continuous presence of high intracellular Zn^{2+} hence, allowing the cancer cells to attain its normal cancerous cell growth rate.

Contradicting findings with regards to the effects of Zn^{2+} on prostate cancer cell growth and invasion have been reported (18,22,63-65). While there are suggestions that dietary zinc supplementation protects against oxidative damage, reduces cancer risk (66) and is beneficial against prostate tumorigenesis (67), recent reports showed that advanced prostate cancer is associated with high intake of zinc (68-70). Higher intake of dietary zinc could also potentiate the development of BPH and progression towards cancer (71,72). These reports raised concern of the potential detrimental outcomes of long-term use of high zinc-supplements in men even though the reason behind the increased in prostate cancer risk is unclear. To date, no satisfactory mechanisms have been forwarded to explain these seemingly contradicting roles of zinc in prostate cancer tumorigenesis. In an earlier study, it was shown that Zn^{2+} deficiency in normal prostate epithelial cells resulted in altered expression of genes associated with cell cycle, DNA damage/repair and gene transcription, suggesting that Zn^{2+} has a protective role in DNA damage and protection against cancer development (15). Results from the present study, however, showed that the LNCaP cells retained its cancerous proliferative rate and properties even though the expression of DNA damage/repair, oxidative stress and apoptosis-related genes are upregulated in the presence of supraphysiologic zinc. This implies that there are potentially other zinc-associated mechanisms involved in the survival of the prostate cancer cells. Results presented here also showed that prostate cancer cell proliferation in the presence of supraphysiologic concentration of Zn^{2+} is accompanied by high expression of *FASN*, *FAD*, *TACSTD1*, *FBL*, *ADRM1*, *E2F3*, *CD164* and *STEAP1* genes. Earlier studies have shown that *CD164* (44) and *TACSTD1* (49) are overexpressed in prostate cancer tissues where Zn^{2+} level is known to be low. While the expressions of these genes are constitutively high in prostatic cancer cells, restoration of high intracellular Zn^{2+} did not reduce their expressions, on the contrary it superinduced the expressions of these genes suggesting that the regulation of these genes by Zn^{2+} is lost irreversibly in prostatic cancer cells. These genes are known to promote prostate cancer cell proliferation, aggressiveness and for some of these genes, the expression is associated with poor survival outcomes of cancer patients. We also found that *CD164*, *FBL* and *TACSTD1* were regulated by Zn^{2+} in normal prostate PNT2 cells and these suggest that while Zn^{2+} initially suppresses cell growth, perhaps by repressing the expressions of selected growth promoting genes, it could also alternatively facilitate the survival of prostate cancer cell through mechanisms involving these very genes, possibly through an autostimulating pathways that superinduce the expression of the genes. Hence, prolonged high Zn^{2+}-treatment could actually induce aggressive behavior of the prostate cancer cells. This suggestion offers a possible explanation to the development of prostate cancer. Perhaps during the very early stages of prostate cancer, the presence of relatively high level of zinc regulates the expression of these genes and only when significant subsequent changes in Zn^{2+} homeostasis occur that it trigger uncontrolled prostate cell growth leading to cancer.

How Zn^{2+} affects *CD164*, *FBL* and *TACSTD1* is still unclear. *CD164* and *TACSTD1* (Ep-CAM) are cell adhesion molecules important for cell migration, proliferation, and differentiation (73,74). *CD164* is implicated in prostate cancer metastasis by promoting the immobilization of cancer cells to bone marrow through the CXCL12/CXCR4 pathway (44). Whereas, fibrillarin (*FBL*), another gene found constitutively high in LNCaP cells and is superinduced by high intracellular Zn^{2+} is a nucleolar U3 ribonucleoprotein particle that is important for pre-rRNA processing during ribosomal biogenesis and maintains nuclear shape and cellular growth (75). *FBL* is also found upregulated in human cervical squamous cell carcinoma (56) and hepatocellular carcinoma (76). *STEAP1*, on the other hand is highly expressed in multiple cancer cells including prostate, bladder, colon, ovarian and Ewing sarcoma (77) and we showed here that its expression in LNCaP cells is ~56-fold higher than in PNT2 prostate normal cells, yet it is not responsive to Zn^{2+} in comparison to other genes studied. *STEAP1* is a transmembrane protein with a potential role in the reduction of copper and iron (78). It is likely therefore, that Zn^{2+} which does not participate in redox reaction (79) may not have an effect on *STEAP1* expression. The mechanisms of how other genes except *STEAP1* are superinduced following long-term high intracellular Zn^{2+} treatment are still unknown. We had previously shown that under similar conditions the Zn^{2+}-regulation of LNCaP cell growth could be mediated through the ERK/VHR/ZAP-70 pathway (23). The finding in the present study that genes such as *C1QBP1* (31), *SHC1* (80),

AHR (81), *ARF4* (82), *RPS6KB2* (83) and *KTN1* (84) are upregulated following Zn^{2+} treatment supported this suggestion, as these genes are known to be regulated through the ERK signaling pathway highlighting the potential importance of this pathway in prostate cancer biogenesis.

Taken together, findings from the present study offer possible explanations to the contradicting reports on the influence of zinc on prostate cancer development. Zn^{2+} may have suppressive effects on prostate cancer cell growth initially but its presence at high level under transformed condition may results in deleterious consequences. Zn^{2+}-based therapy for prostate cancer, hence, may potentially contribute to undesirable outcomes.

Acknowledgements

This study was funded in parts by Program Intensification of Research In Priority Area (IRPA) Grant No. 06-02-03-1025 (Oracle 8361025), University of Malaya short-term research grants VotF-382/2005C and VotF-0173/2003B. P.F. Wong is the recipient of the National Science Fellowship (NSF) Ph.D. Scholarship from the Ministry of Science, Technology and Innovations, Malaysia.

References

1. Vasto S, Candore G, Listi F, Balistreri CR, Colonna-Romano G, Malavolta M, Lio D, Nuzzo D, Mocchegiani E, Di Bona D and Caruso C: Inflammation, genes and zinc in Alzheimer's disease. Brain Res Rev 58: 96-105, 2008.
2. Devirgiliis C, Zalewski PD, Perozzi G and Murgia C: Zinc fluxes and zinc transporter genes in chronic diseases. Mutat Res 622: 84-93, 2007.
3. Donadelli M, Dalla Pozza E, Costanzo C, Scupoli MT, Scarpa A and Palmieri M: Zinc depletion efficiently inhibits pancreatic cancer cell growth by increasing the ratio of antiproliferative/proliferative genes. J Cell Biochem 104: 202-212, 2008.
4. Costello LC, Feng P, Milon B, Tan M and Franklin RB: Role of zinc in the pathogenesis and treatment of prostate cancer: critical issues to resolve. Prostate Cancer Prostatic Dis 7: 111-117, 2004.
5. Kumar A, Chatopadhyay T, Raziuddin M and Ralhan R: Discovery of deregulation of zinc homeostasis and its associated genes in esophageal squamous cell carcinoma using cDNA microarray. Int J Cancer 120: 230-242, 2007.
6. Blanchard RK, Moore JB, Green CL and Cousins RJ: Modulation of intestinal gene expression by dietary zinc status: effectiveness of cDNA arrays for expression profiling of a single nutrient deficiency. Proc Natl Acad Sci USA 98: 13507-13513, 2001.
7. Sun JY, Wang JF, Zi NT, Jing MY and Weng XY: Gene expression profiles analysis of the growing rat liver in response to different zinc status by cDNA microarray analysis. Biol Trace Elem Res 115: 169-185, 2007.
8. Tom Dieck H, Doring F, Roth HP and Daniel H: Changes in rat hepatic gene expression in response to zinc deficiency as assessed by DNA arrays. J Nutr 133: 1004-1010, 2003.
9. Haase H, Mazzatti DJ, White A, Ibs KH, Engelhardt G, Hebel S, Powell JR and Rink L: Differential gene expression after zinc supplementation and deprivation in human leukocyte subsets. Mol Med 13: 362-370, 2007.
10. Aydemir TB, Blanchard RK and Cousins RJ: Zinc supplementation of young men alters metallothionein, zinc transporter, and cytokine gene expression in leukocyte populations. Proc Natl Acad Sci USA 103: 1699-1704, 2006.
11. Cousins RJ, Blanchard RK, Popp MP, Liu L, Cao J, Moore JB and Green CL: A global view of the selectivity of zinc deprivation and excess on genes expressed in human THP-1 mononuclear cells. Proc Natl Acad Sci USA 100: 6952-6957, 2003.
12. Andree KB, Kim J, Kirschke CP, Gregg JP, Paik H, Joung H, Woodhouse L, King JC and Huang L: Investigation of lymphocyte gene expression for use as biomarkers for zinc status in humans. J Nutr 134: 1716-1723, 2004.
13. Beck FW, Li Y, Bao B, Prasad AS and Sarkar FH: Evidence for reprogramming global gene expression during zinc deficiency in the HUT-78 cell line. Nutrition 22: 1045-1056, 2006.
14. Kindermann B, Doring F, Pfaffl M and Daniel H: Identification of genes responsive to intracellular zinc depletion in the human colon adenocarcinoma cell line HT-29. J Nutr 134: 57-62, 2004.
15. Yan M, Song Y, Wong CP, Hardin K and Ho E: Zinc deficiency alters DNA damage response genes in normal human prostate epithelial cells. J Nutr 138: 667-673, 2008.
16. Ebisch IM, Thomas CM, Peters WH, Braat DD and Steegers-Theunissen RP: The importance of folate, zinc and antioxidants in the pathogenesis and prevention of subfertility. Hum Reprod Update 13: 163-174, 2007.
17. Zaichick V, Sviridova TV and Zaichick SV: Zinc in the human prostate gland: normal, hyperplastic and cancerous. Int Urol Nephrol 29: 565-574, 1997.
18. Uzzo RG, Crispen PL, Golovine K, Makhov P, Horwitz EM and Kolenko VM: Diverse effects of zinc on NF-kappaB and AP-1 transcription factors: implications for prostate cancer progression. Carcinogenesis 27: 1980-1990, 2006.
19. Gioeli D: Signal transduction in prostate cancer progression. Clin Sci (London) 108: 293-308, 2005.
20. Feng P, Li TL, Guan ZX, Franklin RB and Costello LC: Direct effect of zinc on mitochondrial apoptogenesis in prostate cells. Prostate 52: 311-318, 2002.
21. Ishii K, Usui S, Sugimura Y, Yamamoto H, Yoshikawa K and Hirano K: Inhibition of aminopeptidase N (AP-N) and urokinase-type plasminogen activator (uPA) by zinc suppresses the invasion activity in human urological cancer cells. Biol Pharm Bull 24: 226-230, 2001.
22. Boissier S, Ferreras M, Peyruchaud O, Magnetto S, Ebetino FH, Colombel M, Delmas P, Delaisse JM and Clezardin P: Bisphosphonates inhibit breast and prostate carcinoma cell invasion, an early event in the formation of bone metastases. Cancer Res 60: 2949-2954, 2000.
23. Wong PF and Abubakar S: High intracellular Zn^{2+} ions modulate the VHR, ZAP-70 and ERK activities of LNCaP prostate cancer cells. Cell Mol Biol Lett 13: 375-390, 2008.
24. Wong PF and Abubakar S: LNCaP prostate cancer cells are insensitive to zinc-induced senescence. J Trace Elem Med Biol 22: 242-247, 2008.
25. Benjamini Y and Hochberg Y: Controlling the false discovery rate: a practical and powerful approach to multiple testing. J R Stat Soc Series B (Methodological) 57: 289-300, 1995.
26. Beisvag V, Junge FK, Bergum H, Jolsum L, Lydersen S, Gunther CC, Ramampiaro H, Langaas M, Sandvik AK and Laegreid A: GeneTools- application for functional annotation and statistical hypothesis testing. BMC Bioinformatics 7: 470, 2006.
27. Huggett J, Dheda K, Bustin S and Zumla A: Real-time RT-PCR normalisation, strategies and considerations. Genes Immun 6: 279-284, 2005.
28. Rouault JP, Falette N, Guehenneux F, Guillot C, Rimokh R, Wang Q, Berthet C, Moyret-Lalle C, Savatier P, Pain B, Shaw P, Berger R, Samarut J, Magaud JP, Ozturk M, Samarut C and Puisieux A: Identification of BTG2, an antiproliferative p53-dependent component of the DNA damage cellular response pathway. Nat Genet 14: 482-486, 1996.
29. Ohtsuka T, Ryu H, Minamishima YA, Ryo A and Lee SW: Modulation of p53 and p73 levels by cyclin G: implication of a negative feedback regulation. Oncogene 22: 1678-1687, 2003.
30. Machida T, Fujita T, Ooo ML, Ohira M, Isogai E, Mihara M, Hirato J, Tomotsune D, Hirata T, Fujimori M, Adachi W and Nakagawara A: Increased expression of proapoptotic BMCC1, a novel gene with the BNIP2 and Cdc42GAP homology (BCH) domain, is associated with favorable prognosis in human neuroblastomas. Oncogene 25: 1931-1942, 2006.
31. Meenakshi J, Anupama, Goswami SK and Datta K: Constitutive expression of hyaluronan binding protein 1 (HABP1/p32/ gC1qR) in normal fibroblast cells perturbs its growth characteristics and induces apoptosis. Biochem Biophys Res Commun 300: 686-693, 2003.

H, Lee JC, Moon HJ, Jung JE, Sharma M, Park BH, and Jhee EC: Differential effect of oxidative stress on the apoptosis of early and late passage human diploid fibroblasts: implication of heat shock protein 60. Cell Biochem Funct 26: 502-508, 2008.
33. Budanov AV, Shoshani T, Faerman A, Zelin E, Kamer I, Kalinski H, Gorodin S, Fishman A, Chajut A, Einat P, Skaliter R, Gudkov AV, Chumakov PM and Feinstein E: Identification of a novel stress-responsive gene Hi95 involved in regulation of cell viability. Oncogene 21: 6017-6031, 2002.
34. Ramsden JJ: MARCKS: a case of molecular exaptation? Int J Biochem Cell Biol 32: 475-479, 2000.
35. Martinez-Arribas F, Agudo D, Pollan M, Gomez-Esquer F, Diaz-Gil G, Lucas R and Schneider J: Positive correlation between the expression of X-chromosome RBM genes (RBMX, RBM3, RBM10) and the proapoptotic Bax gene in human breast cancer. J Cell Biochem 97: 1275-1282, 2006.
36. Jin R, Huang J, Tan PH and Bay BH: Clinicopathological significance of metallothioneins in breast cancer. Pathol Oncol Res 10: 74-79, 2004.
37. Tiberi L, Faisal A, Rossi M, Di Tella L, Franceschi C and Salvioli S: p66(Shc) gene has a pro-apoptotic role in human cell lines and it is activated by a p53-independent pathway. Biochem Biophys Res Commun 342: 503-508, 2006.
38. Iwanaga R, Komori H and Ohtani K: Differential regulation of expression of the mammalian DNA repair genes by growth stimulation. Oncogene 23: 8581-8590, 2004.
39. Kanu N and Behrens A: ATMINistrating ATM signalling: regulation of ATM by ATMIN. Cell Cycle 7: 3483-3486, 2008.
40. Bladen CL, Udayakumar D, Takeda Y and Dynan WS: Identification of the polypyrimidine tract binding protein-associated splicing factor.p54(nrb) complex as a candidate DNA double-strand break rejoining factor. J Biol Chem 280: 5205-5210, 2005.
41. Singh R, Lemire J, Mailloux RJ and Appanna VD: A novel strategy involved anti-oxidative defense: the conversion of NADH into NADPH by a metabolic network. PLoS One 3: e2682, 2008.
42. Lu DD, Chen YC, Zhang XR, Cao XR, Jiang HY and Yao L: The relationship between metallothionein-1F (MT1F) gene and hepatocellular carcinoma. Yale J Biol Med 76: 55-62, 2003.
43. Hellborg F, Qian W, Mendez-Vidal C, Asker C, Kost-Alimova M, Wilhelm M, Imreh S and Wiman KG: Human wig-1, a p53 target gene that encodes a growth inhibitory zinc finger protein. Oncogene 20: 5466-5474, 2001.
44. Havens AM, Jung Y, Sun YX, Wang J, Shah RB, Buhring HJ, Pienta KJ and Taichman RS: The role of sialomucin CD164 (MGC-24v or endolyn) in prostate cancer metastasis. BMC Cancer 6: 195, 2006.
45. Rossi S, Graner E, Febbo P, Weinstein L, Bhattacharya N, Onody T, Bubley G, Balk S and Loda M: Fatty acid synthase expression defines distinct molecular signatures in prostate cancer. Mol Cancer Res 1: 707-715, 2003.
46. Moore S, Knudsen B, True LD, Hawley S, Etzioni R, Wade C, Gifford D, Coleman I and Nelson PS: Loss of stearoyl-CoA desaturase expression is a frequent event in prostate carcinoma. Int J Cancer 114: 563-571, 2005.
47. Ishiguro H, Uemura H, Fujinami K, Ikeda N, Ohta S and Kubota Y: 55 kDa nuclear matrix protein (nmt55) mRNA is expressed in human prostate cancer tissue and is associated with the androgen receptor. Int J Cancer 105: 26-32, 2003.
48. Bogni A, Cheng C, Liu W, Yang W, Pfeffer J, Mukatira S, French D, Downing JR, Pui CH and Relling MV: Genome-wide approach to identify risk factors for therapy-related myeloid leukemia. Leukemia 20: 239-246, 2006.
49. Went P, Vasei M, Bubendorf L, Terracciano L, Tornillo L, Riede U, Kononen J, Simon R, Sauter G and Baeuerle PA: Frequent high-level expression of the immunotherapeutic target Ep-CAM in colon, stomach, prostate and lung cancers. Br J Cancer 94: 128-135, 2006.
50. Lapointe J, Li C, Higgins JP, van de Rijn M, Bair E, Montgomery K, Ferrari M, Egevad L, Rayford W, Bergerheim U, Ekman P, DeMarzo AM, Tibshirani R, Botstein D, Brown PO, Brooks JD and Pollack JR: Gene expression profiling identifies clinically relevant subtypes of prostate cancer. Proc Natl Acad Sci USA 101: 811-816, 2004.
51. Rasheed S, Harris AL, Tekkis PP, Turley H, Silver A, McDonald PJ, Talbot IC, Glynne-Jones R, Northover JM and Guenther T: Hypoxia-inducible factor-1alpha and -2alpha are expressed in most rectal cancers but only hypoxia-inducible factor-1alpha is associated with prognosis. Br J Cancer 100: 1666-1673, 2009.
52. Mollaoglu N, Vairaktaris E, Nkenke E, Neukam FW and Ries J: Expression of MAGE-A12 in oral squamous cell carcinoma. Dis Markers 24: 27-32, 2008.
53. Vaarala MH, Porvari KS, Kyllonen AP, Mustonen MV, Lukkarinen O and Vihko PT: Several genes encoding ribosomal proteins are over-expressed in prostate-cancer cell lines: confirmation of L7a and L37 over-expression in prostate-cancer tissue samples. Int J Cancer 78: 27-32, 1998.
54. Bai L and Merchant JL: A role for CITED2, a CBP/p300 interacting protein, in colon cancer cell invasion. FEBS Lett 581: 5904-5910, 2007.
55. He H, Dai F, Yu L, She X, Zhao Y, Jiang J, Chen X and Zhao S: Identification and characterization of nine novel human small GTPases showing variable expressions in liver cancer tissues. Gene Expr 10: 231-242, 2002.
56. Choi YW, Kim YW, Bae SM, Kwak SY, Chun HJ, Tong SY, Lee HN, Shin JC, Kim KT, Kim YJ and Ahn WS: Identification of differentially expressed genes using annealing control primer-based GeneFishing in human squamous cell cervical carcinoma. Clin Oncol (R Coll Radiol) 19: 308-318, 2007.
57. Suzuki S, Takahashi S, Takeshita K, Hikosaka A, Wakita T, Nishiyama N, Fujita T, Okamura T and Shirai T: Expression of prothymosin alpha is correlated with development and progression in human prostate cancers. Prostate 66: 463-469, 2006.
58. Rizzi F, Belloni L, Crafa P, Lazzaretti M, Remondini D, Ferretti S, Cortellini P, Corti A and Bettuzzi S: A novel gene signature for molecular diagnosis of human prostate cancer by RT-qPCR. PLoS One 3: e3617, 2008.
59. Dunn TA, Chen S, Faith DA, Hicks JL, Platz EA, Chen Y, Ewing CM, Sauvageot J, Isaacs WB, De Marzo AM and Luo J: A novel role of myosin VI in human prostate cancer. Am J Pathol 169: 1843-1854, 2006.
60. Aerts JL, Gonzales MI and Topalian SL: Selection of appropriate control genes to assess expression of tumor antigens using real-time RT-PCR. Biotechniques 36: 84-91, 2004.
61. Vandesompele J, De Preter K, Pattyn F, Poppe B, Van Roy N, De Paepe A and Speleman F: Accurate normalization of real-time quantitative RT-PCR data by geometric averaging of multiple internal control genes. Genome Biol 3: Research0034, 2002.
62. Albrecht AL, Somji S, Sens MA, Sens DA and Garrett SH: Zinc transporter mRNA expression in the RWPE-1 human prostate epithelial cell line. Biometals 21: 405-416, 2008.
63. Feng P, Liang JY, Li TL, Guan ZX, Zou J, Franklin R and Costello LC: Zinc induces mitochondria apoptogenesis in prostate cells. Mol Urol 4: 31-36, 2000.
64. Ishii K, Otsuka T, Iguchi K, Usui S, Yamamoto H, Sugimura Y, Yoshikawa K, Hayward SW and Hirano K: Evidence that the prostate-specific antigen (PSA)/Zn^{2+} axis may play a role in human prostate cancer cell invasion. Cancer Lett 207: 79-87, 2004.
65. Nemoto K, Kondo Y, Himeno S, Suzuki Y, Hara S, Akimoto M and Imura N: Modulation of telomerase activity by zinc in human prostatic and renal cancer cells. Biochem Pharmacol 59: 401-405, 2000.
66. Ho E: Zinc deficiency, DNA damage and cancer risk. J Nutr Biochem 15: 572-578, 2004.
67. Franklin RB and Costello LC: Zinc as an anti-tumor agent in prostate cancer and in other cancers. Arch Biochem Biophys 463: 211-217, 2007.
68. Gallus S, Foschi R, Negri E, Talamini R, Franceschi S, Montella M, Ramazzotti V, Tavani A, Dal Maso L and La Vecchia C: Dietary zinc and prostate cancer risk: a case-control study from Italy. Eur Urol 52: 1052-1056, 2007.
69. Lawson KA, Wright ME, Subar A, Mouw T, Hollenbeck A, Schatzkin A and Leitzmann MF: Multivitamin use and risk of prostate cancer in the National Institutes of Health-AARP Diet and Health Study. J Natl Cancer Inst 99: 754-764, 2007.
70. Leitzmann MF, Stampfer MJ, Wu K, Colditz GA, Willett WC and Giovannucci EL: Zinc supplement use and risk of prostate cancer. J Natl Cancer Inst 95: 1004-1007, 2003.
71. Lagiou P, Wuu J, Trichopoulou A, Hsieh CC, Adami HO and Trichopoulos D: Diet and benign prostatic hyperplasia: a study in Greece. Urology 54: 284-290, 1999.

72. Moyad MA: Zinc for prostate disease and other conditions: a little evidence, a lot of hype, and a significant potential problem. Urol Nurs 24: 49-52, 2004.
73. Zannettino AC, Buhring HJ, Niutta S, Watt SM, Benton MA and Simmons PJ: The sialomucin CD164 (MGC-24v) is an adhesive glycoprotein expressed by human hematopoietic progenitors and bone marrow stromal cells that serves as a potent negative regulator of hematopoiesis. Blood 92: 2613-2628, 1998.
74. Trzpis M, McLaughlin PM, de Leij LM and Harmsen MC: Epithelial cell adhesion molecule: more than a carcinoma marker and adhesion molecule. Am J Pathol 171: 386-395, 2007.
75. Amin MA, Matsunaga S, Ma N, Takata H, Yokoyama M, Uchiyama S and Fukui K: Fibrillarin, a nucleolar protein, is required for normal nuclear morphology and cellular growth in HeLa cells. Biochem Biophys Res Commun 360: 320-326, 2007.
76. Zhang JY, Wang X, Peng XX and Chan EK: Autoantibody responses in Chinese hepatocellular carcinoma. J Clin Immunol 22: 98-105, 2002.
77. Hubert RS, Vivanco I, Chen E, Rastegar S, Leong K, Mitchell SC, Madraswala R, Zhou Y, Kuo J, Raitano AB, Jakobovits A, Saffran DC and Afar DE: STEAP: a prostate-specific cell-surface antigen highly expressed in human prostate tumors. Proc Natl Acad Sci USA 96: 14523-14528, 1999.
78. Ohgami RS, Campagna DR, McDonald A and Fleming MD: The Steap proteins are metalloreductases. Blood 108: 1388-1394, 2006.
79. Berg JM and Shi Y: The galvanization of biology: a growing appreciation for the roles of zinc. Science 271: 1081-1085, 1996.
80. Arany I, Faisal A, Nagamine Y and Safirstein RL: p66shc inhibits pro-survival epidermal growth factor receptor/ERK signaling during severe oxidative stress in mouse renal proximal tubule cells. J Biol Chem 283: 6110-6117, 2008.
81. Hanlon PR, Ganem LG, Cho YC, Yamamoto M and Jefcoate CR: AhR- and ERK-dependent pathways function synergistically to mediate 2,3,7,8-tetrachlorodibenzo-p-dioxin suppression of peroxisome proliferator-activated receptor-gamma1 expression and subsequent adipocyte differentiation. Toxicol Appl Pharmacol 189: 11-27, 2003.
82. Kim SW, Hayashi M, Lo JF, Yang Y, Yoo JS and Lee JD: ADP-ribosylation factor 4 small GTPase mediates epidermal growth factor receptor-dependent phospholipase D2 activation. J Biol Chem 278: 2661-2668, 2003.
83. Casas-Terradellas E, Tato I, Bartrons R, Ventura F and Rosa JL: ERK and p38 pathways regulate amino acid signalling. Biochim Biophys Acta 1783: 2241-2254, 2008.
84. Hotta K, Tanaka K, Mino A, Kohno H and Takai Y: Interaction of the Rho family small G proteins with kinectin, an anchoring protein of kinesin motor. Biochem Biophys Res Commun 225: 69-74, 1996.